

Towards a Connection Between Nuclear Structure and QCD

Anthony W. THOMAS^{1,2}, Pierre A. M. GUICHON³, Derek B. LEINWEBER²
and Ross D. YOUNG²

¹*Jefferson Lab, 12000 Jefferson Ave., Newport News VA 23606 USA*

²*Centre for the Subatomic Structure of Matter and*

Department of Physics, University of Adelaide, Adelaide SA 5005, Australia

³*SPhN-DAPNIA, CEA Saclay, F91191 Gif sur Yvette, France*

As we search for an ever deeper understanding of the structure of hadronic matter one of the most fundamental questions is whether or not one can make a connection to the underlying theory of the strong interaction, QCD. We build on recent advances in the chiral extrapolation problem linking lattice QCD at relatively large “light quark” masses to the physical world to estimate the scalar polarizability of the nucleon. The latter plays a key role in modern relativistic mean-field descriptions of nuclei and nuclear matter (such as QMC) and, in particular, leads to a very natural saturation mechanism. We demonstrate that the value of the scalar polarizability extracted from the lattice data is consistent with that needed for a successful description of nuclei within the framework of QMC. In a very real sense this is the first hint of a direct connection between QCD and the properties of finite nuclei.

§1. Introduction

Over the century since Rutherford made the first discovery concerning nuclear structure, understanding the mechanism for nuclear saturation has been a central concern. Within the traditional framework of many-body theory based on two-body potentials, strong short-distance repulsion was the key. The importance of relativity was made clear within quantum-hydrodynamics (QHD), with the scalar density of nucleons (which determines the attractive scalar, σ -meson, coupling) growing more slowly than the density (which in turn determines the repulsive vector, ω -meson, coupling).

Since the discovery of QCD as the fundamental theory of the strong interaction, numerous attempts have been made to derive the NN force within quark models. Fewer attempts have been made to understand nuclear structure at the quark level.^{1),2)} The quark-meson coupling (QMC) model³⁾⁻⁶⁾ stands between the traditional meson-exchange picture and the hard core quark models. It is a mean field model in the sense of QHD but with the σ and ω mesons coupling to confined quarks, rather than to point-like nucleons. In the simple case of infinite nuclear matter, after a considerable amount of work, one finds that the only effect of the internal, quark structure of the nucleons is that the σ -nucleon coupling becomes density dependent. That is, the nucleon effective mass takes the form:

$$M_N^* = M_N - g_\sigma(\sigma)\sigma \quad (1.1)$$

where $g_\sigma(\sigma) \approx g_\sigma + g_{\sigma\sigma}\sigma$, g_σ is the coupling at zero density and $g_{\sigma\sigma}$ is known as the scalar polarizability.^{3),6)-8)}

If the MIT bag model is used to describe the quark confinement (as in the original QMC model) the scalar polarizability is negative, that is it tends to oppose the applied scalar field. Indeed, one finds $g_{\sigma\sigma} = -0.11g_{\sigma}R$, with R the bag radius. A similar result is found in the NJL model,⁷⁾ once it is modified to simulate the effect of confinement⁹⁾ – a change which also resolves the long standing question of chiral collapse in the NJL model.

The crucial point is now that a negative scalar polarizability (associated with a readjustment of the internal, quark structure of the nucleon in response to an applied scalar field) is all that is needed to lead to the saturation of the binding energy of nuclear matter as a function of density. In contrast with the Walecka model (QHD),¹⁰⁾ where the σ -nucleon coupling really is a constant, the mean scalar and vector fields at nuclear matter density are much smaller because one is not relying on a difference between $\bar{\psi}_N\psi_N$ and $\psi_N^\dagger\psi_N$ arising from relativistic motion of the bound nucleons.

While the situation just described is somewhat simplistic as a description of nuclear saturation, it is certainly sufficient. Moreover, it has recently been shown that a systematic expansion of the QMC model as a function of density allows a direct comparison with the widely used Skyrme effective forces.¹¹⁾ In that framework one can also include anti-symmetrization at the nucleon level, leading to new values of the σ and ω coupling constants. With these values the expansion of the effective model as an effective nuclear force yields agreement at the 10% level. This provides a remarkable indication of the role of confined quarks in even low energy nuclear physics.

§2. The Status of Chiral Extrapolation for the Mass of the Nucleon

The challenge of solving a strongly coupled field theory with spontaneous symmetry breaking is central to understanding the strong interaction within the Standard Model. It will be quite a few years before full QCD simulations can be performed at physical light quark masses – with computation time scaling like $\sim 1/m_q^{3.6}$,¹²⁾ quark masses are typically restricted to above 50 MeV for accurate calculations with improved quark and gluon actions. The exception to this is to use staggered fermions, which have shown some results at 25 MeV,¹³⁾ but this approach has a number of technical problems, including multiple pions (extra tastes) – which complicate the chiral extrapolation problem which we explore next.

Given that one cannot directly calculate hadron properties at realistic quark masses, if one wishes to make any connection with experimental data it is necessary to find an appropriate method to extrapolate the properties calculated at large *light-quark* mass to the physical value. This is the chiral extrapolation problem, which is complicated by spontaneous chiral symmetry breaking in QCD. As we shall explain, this problem has recently been solved by a careful reformulation of the effective field theory.

The power of effective field theory for strongly interacting systems has been apparent for more than 50 years, beginning with Foldy's inclusion of the anomalous magnetic moment of the proton in a derivative expansion of the electromagnetic

coupling of photons to baryons. Of course, the fact that nucleon form factors can be approximated by a dipole with mass parameter $M^2 = 0.71 \text{ GeV}^2$ means that the radius of convergence of the formal expansion is less than 0.84 GeV . In the last twenty years our understanding of the symmetries of QCD have led to a systematic expansion of hadron properties and scattering amplitudes about the limits $m_\pi = 0$ and $q = 0$, known as chiral perturbation theory. For the pseudoscalar mesons, which are rigorously massless in the limit where the u , d and s quark masses are zero (the chiral $SU(3)$ limit), this approach has been especially successful. Although, even here, serious questions have been raised over whether the formal expansion is really convergent for masses as large as m_s .^{14)–16)}

For our immediate interest in the scalar polarizability of the nucleon, we shall concentrate on understanding the dependence of M_N on light quark mass m_q . Given the Gell-Mann–Oakes–Renner (GMOR) relation, $m_\pi^2 \propto m_q$, we prefer to use m_π^2 , rather than m_q , as the measure of explicit chiral symmetry breaking in the expressions below. (We stress, however, that wherever the GMOR relation fails, e.g. for $m_\pi^2 > 0.8 \text{ GeV}^2$ or for $m_\pi \rightarrow 0$ in QQCD (where there are logarithmic chiral corrections to GMOR), one should revert to an expansion written explicitly in terms of m_q .) The formal chiral expansion for M_N , in terms of m_π , about the $SU(2)$ chiral limit in full QCD is:

$$M_N = a_0 + a_2 m_\pi^2 + a_4 m_\pi^4 + a_6 m_\pi^6 + \dots \\ + \sigma_{N\pi}(m_\pi) + \sigma_{\Delta\pi}(m_\pi), \quad (2.1)$$

where $\sigma_{B\pi}$ is the self-energy arising from a $B\pi$ loop (with $B = N$ or Δ). These N and Δ loops generate the leading and next-to-leading non-analytic (LNA and NLNA) behaviour, respectively. Note that for the present we have omitted the tadpole term which also contributes at NLNA order. It adds complications which are unimportant for the present discussion – for details we refer to Sec. 2.3 and to Ref.¹⁸⁾

These loop integrals contain ultraviolet divergences which require some regularisation prescription. The standard approach is to use dimensional regularisation to evaluate the self-energy integrals. Under such a scheme the $NN\pi$ contribution simply becomes $\sigma_{N\pi}(m_\pi) \rightarrow c_{\text{LNA}} m_\pi^3$ and the analytic terms, a_0 and $a_2 m_\pi^2$, undergo an infinite renormalisation. The Δ contribution produces a logarithm, so that the complete series expansion of the nucleon mass about $m_\pi = 0$ is:

$$M_N = c_0 + c_2 m_\pi^2 + c_4 m_\pi^4 + c_{\text{LNA}} m_\pi^3 + c_{\text{NLNA}} m_\pi^4 \log m_\pi + \dots, \quad (2.2)$$

where the a_i have been replaced by the renormalised (and finite) parameters c_i .

The coefficients of the low-order, non-analytic contributions are known:^{19)–21)}

$$c_{\text{LNA}} = -\frac{3}{32\pi f_\pi^2} g_A^2, \quad c_{\text{NLNA}} = \frac{3}{32\pi f_\pi^2} \frac{32}{25} g_A^2 \frac{3}{4\pi\Delta}. \quad (2.3)$$

Although strictly one should use values in the chiral limit, we take the experimental numbers with $g_A = 1.26$, $f_\pi = 0.093 \text{ GeV}$, the $N - \Delta$ mass splitting, $\Delta = 0.292 \text{ GeV}$ and the mass scale associated with the logarithms will be taken to be 1 GeV .

We stress that whereas Eq. (2.2) was derived in the limit $m_\pi/\Delta \ll 1$, at just twice the physical pion mass this ratio approaches unity. Mathematically the region

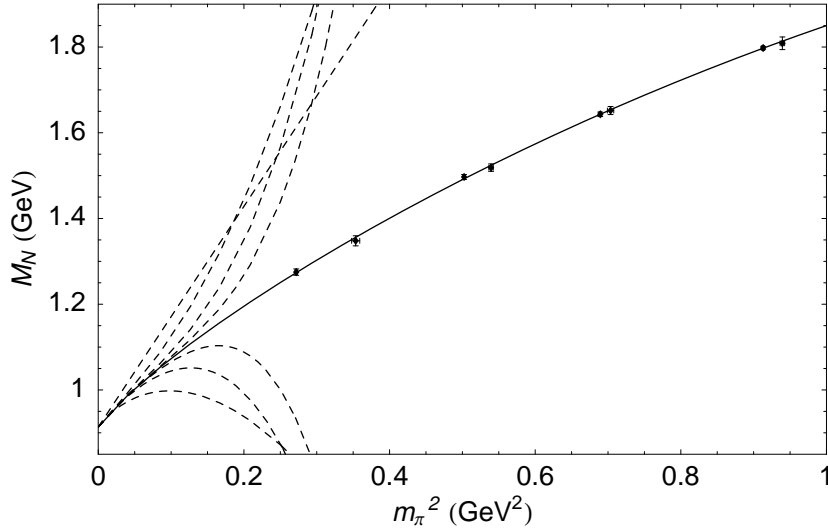


Fig. 1. Fits to lattice data with dipole regulator for the self-energy loop $N \rightarrow N\pi$ (neglecting the $N \rightarrow \Delta\pi$ term for simplicity). The dashed lines show the expansion up to successive orders in m_π , from m_π^2 up to m_π^8 – these alternate about the solid curve as we go through even and odd terms.

$m_\pi \approx \Delta$ is dominated by a square root branch cut which starts at $m_\pi = \Delta$. Using dimensional regularisation this takes the form:²²⁾

$$\frac{-3}{32\pi} \frac{32}{f_\pi^2} \frac{g_A^2}{25} \frac{1}{2\pi} \left[(2\Delta^3 - 3m_\pi^2 \Delta) \log\left(\frac{m_\pi^2}{\mu^2}\right) - 2(\Delta^2 - m_\pi^2)^{\frac{3}{2}} \log\left(\frac{\Delta - \sqrt{\Delta^2 - m_\pi^2}}{\Delta + \sqrt{\Delta^2 - m_\pi^2}}\right) \right] \quad (2.4)$$

for $m_\pi < \Delta$, while for $m_\pi > \Delta$ the second logarithm becomes an arctangent. Clearly, to access the higher quark masses in the chiral expansion, currently of most relevance to lattice QCD, one requires a more sophisticated expression than that given by Eq. (2.2).

2.1. Issues of convergence

Forgetting for a moment the issues surrounding the $\Delta\pi$ cut, we note that the formal expansion of the $N \rightarrow N\pi \rightarrow N$ self-energy integral, $\sigma_{N\pi}$, has been shown to have poor convergence properties. Using a sharp, ultra-violet cut-off, Wright showed²³⁾ that the series expansion, truncated at $\mathcal{O}(m_\pi^4)$, diverged for $m_\pi > 0.4$ GeV. This already indicated that the series expansion motivated by dimensional regularisation would have a slow rate of convergence. A similar conclusion had been reached somewhat earlier by Stuckey and Birse.¹⁷⁾

In considering the convergence of the truncated series, Eq. (2.2), it is helpful to return to the general form from which it was derived, namely Eq. (2.1). The dimensionally regulated approach requires that the pion mass should remain much lighter than every other mass scale involved in the problem. This requires that $m_\pi/\Lambda_{\chi\text{SB}} \ll 1$ (and $m_\pi/\Delta \ll 1$ if we use the simple logarithm in Eq.(2.2) rather than the full cut structure of Eq.(2.4)).

An additional mass scale, which we address in detail below, is set by the physical

extent of the source of the pion field.²⁴⁾ This scale, which is of order R_{SOURCE}^{-1} , corresponds to the transition between the rapid, non-linear variation required by chiral symmetry and the smooth, *constituent-quark* like mass behaviour observed in lattice simulations at larger quark mass. An alternative to dimensional regularisation is to regulate Eq. (2.1) with a finite ultra-violet cut-off in momentum space.

General considerations in effective field theory, as discussed for example by LePage,²⁵⁾ suggest that one should *not* take the cut-off to ∞ . That is, one should not use dimensional regularization. Nor should one attempt to determine the “true” cut-off of the theory. Rather, one should choose a cut-off scale somewhat below the place where the effective theory omits essential physics and use data to constrain the renormalization constants of the theory and hence eliminate the dependence on that cut-off as far as possible.

The issue is then what mass scale determines the upper limit beyond which the effective field theory is applicable. This is commonly taken to be $\Lambda_{\chi PT} \sim 4\pi f_\pi \sim 1$ GeV. Unfortunately this is incorrect for baryons. In the context of nuclear physics it has long been appreciated that nuclear sizes could never be derived from naive dispersion relation considerations of nearest t-channel poles – anomalous thresholds associated with the internal structure of nuclei dominate. Similarly, the size of a baryon is determined by nonperturbative QCD beyond the scope of chiral perturbation theory. The natural scale associated with the size of a nucleon is the inverse of its radius or a mass scale $R_{SOURCE}^{-1} \sim 0.2$ to 0.5 GeV – far below $\Lambda_{\chi PT}$. In the context of effective field theory it is inconsistent to keep loop contributions from momenta above this scale!

As a result of these considerations, we are led to regulate the radiative corrections which give rise to the leading and next-to-leading non-analytic contributions to the mass of the nucleon using a finite range regulator with a mass in the range R_{SOURCE}^{-1} . As far as possible residual dependence on the specific choice of mass scale (and form of regulator function) will be eliminated by fitting the renormalization constants to nonperturbative QCD – in this case data obtained from lattice QCD simulations. The quantitative success of applying the method is to be judged by the extent to which physical results extracted from the analysis are indeed independent of the regulator (over a physically sensible range). We refer to this approach as *finite range regularization*, FRR.

2.2. Analysis of lattice QCD data

In our analysis we have taken as input both the physical nucleon mass and recent lattice QCD results of the CP-PACS Collaboration²⁶⁾ and the JLQCD Collaboration.²⁷⁾ This enables us to constrain an expression for M_N as a function of the quark mass. The lattice results of Ref.²⁶⁾ have been obtained using improved gluon and quark actions on fine, large volume lattices with high statistics. These simulations were performed using an Iwasaki gluon action²⁸⁾ and the mean-field improved clover fermion action. In this work we concentrate on only those results with $m_{sea} = m_{val}$ and the two largest values of β (i.e., the finest lattice spacings $a \sim 0.09 - 0.13$ fm). We use just the largest volume results of Ref.,²⁷⁾ where simulations were performed with non-perturbatively improved Wilson quark action and plaquette gauge action.

The lattice volumes and spacings are similar for the two data sets.

We chose to set the physical scale at each quark mass using the UKQCD method.²⁹⁾ That is, we use the Sommer scale $r_0 = 0.5 \text{ fm}$.^{30),31)} This choice is ideal in the present context because the static quark potential is insensitive to chiral physics. This ensures that the results obtained represent accurate estimates of the continuum, infinite-volume theory at the simulated quark masses. The lattice data lies in the intermediate mass region, with m_π^2 between 0.3 and 1.0 GeV².

Based on Eq. (2.1) we evaluate the loop integrals $\sigma_{N\pi} \equiv c_{LNA} I_\pi(m_\pi, \Lambda)$ and $\sigma_{\Delta\pi} \equiv c_{NLNA} I_{\pi\Delta}(m_\pi, \Lambda)$, where:

$$I_\pi = \frac{2}{\pi} \int_0^\infty dk \frac{k^4 u^2(k)}{k^2 + m^2} \quad (2.5)$$

and

$$I_{\pi\Delta} = -\frac{8\Delta}{3} \int_0^\infty dk \frac{k^4 u^2(k)}{\sqrt{k^2 + m^2}(\Delta + \sqrt{k^2 + m^2})}. \quad (2.6)$$

We use four different functional forms for the finite-ranged, ultra-violet vertex regulator, $u(k)$ — namely the sharp-cutoff (SC), $\theta(\Lambda - k)$; monopole (MON), $\Lambda^2/(\Lambda^2 + k^2)$; dipole (DIP), $\Lambda^4/(\Lambda^2 + k^2)^2$; and Gaussian (GAU), $\exp(-k^2/\Lambda^2)$. Closed expressions for these integrals in the first three cases are given in the Appendix of Ref.³²⁾ Provided one regulates the effective field theory below the point where new short distance physics becomes important, the essential results will not depend on the cut-off scale.²⁵⁾ We use knowledge learned in Ref.³²⁾ as a guide for the appropriate scales for each of the regulator forms.

We have fit the set of lattice data discussed above with the chiral expansions based on six different regularisation prescriptions. In all schemes we allowed the coefficients of the analytic terms up to m_π^6 to be determined by the lattice data. The regulator masses are once again fixed to their preferred values. The best fits, shown in Fig. 2, serve to highlight the remarkable agreement between all finite-range parameterisations. This demonstrates that the extrapolation can be reliably performed using FRR with negligible dependence on the choice of regulator.

In view of the general discussion presented earlier, it is important to check the residual dependence on the choice of cutoff scale Λ . The resulting variation of the extrapolated nucleon mass, at the physical pion mass, for dipole masses ranging from 0.6 to 1.0 GeV is shown in Fig. 3. We see that the residual uncertainty introduced by the cutoff scale is less than 2%, which is insignificant compared to the statistical error in extrapolating such a large distance. With the present data this statistical error is found to be around 13%.

2.3. Complete analysis of the nucleon mass

Here we summarise the results of the most recent and complete analysis of Ref.¹⁸⁾ Including the tadpole term, the nucleon mass has the formal expansion:

$$M_N = a_0 + a_2 m_\pi^2 + a_4 m_\pi^4 + a_6 m_\pi^6 + \sigma_{NN}^\pi + \sigma_{N\Delta}^\pi + \sigma_{\text{tad}}^\pi. \quad (2.7)$$

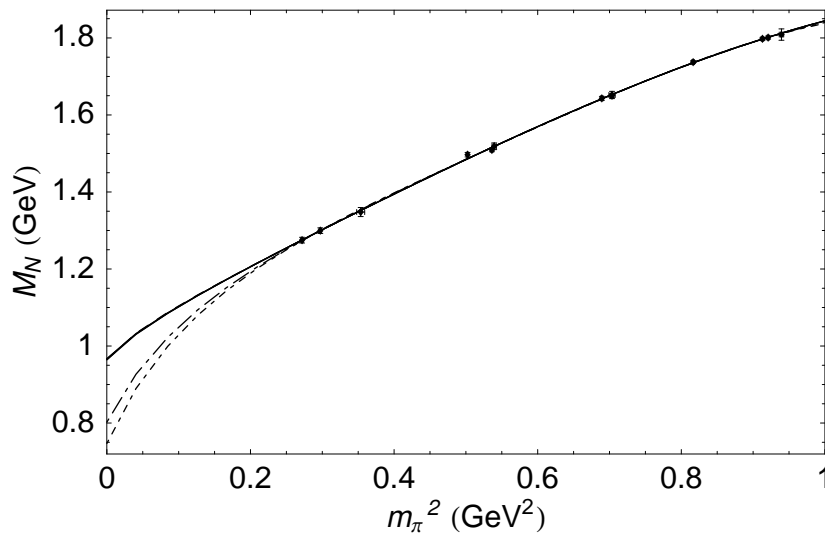


Fig. 2. Extrapolation of lattice data for various regularisations prescriptions, without the tadpole term. The four **indistinguishable**, solid curves show the fits based on four different FRRs. The short dash-dot curve corresponds to the dimensionally regulated case and the long dash-dot curve to that where the branch point in Eq. (2.4) is included in dimensional regularisation.

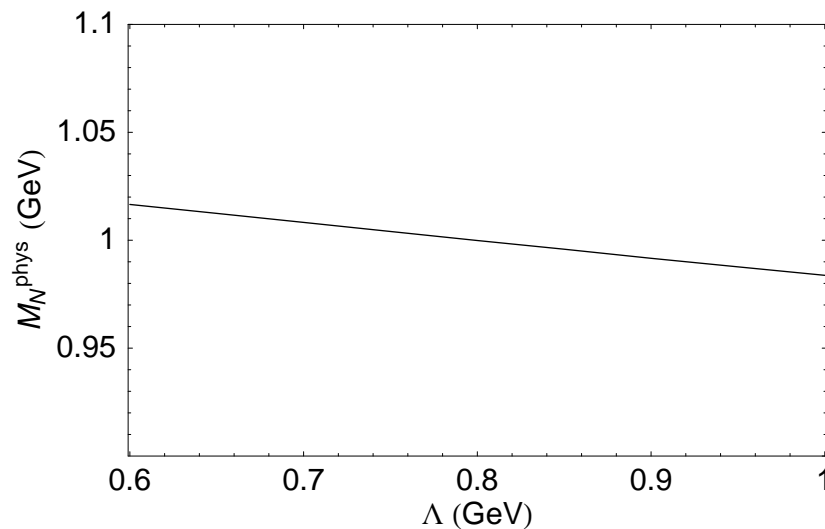


Fig. 3. Illustration of the relatively weak dependence of the extrapolated nucleon mass on the choice of dipole regulator mass, Λ .

As explained earlier, within dimensional regularisation this leads to a truncated power series for the chiral expansion,

$$M_N = c_0 + c_2 m_\pi^2 + c_{\text{LNA}} m_\pi^3 + c_4 m_\pi^4 + c_{\text{NLNA}} m_\pi^4 \ln \frac{m_\pi}{\mu} + c_6 m_\pi^6 + \dots, \quad (2.8)$$

where the bare parameters, a_i , have been replaced by the finite, renormalised coefficients, c_i . Through the chiral logarithm one has an additional mass scale, μ , but

the dependence on this is eliminated by matching c_4 to “data” (in this case lattice QCD). We work to fourth order in the chiral expansion and include the next analytic term to compensate short distance physics contained in the NLNA loop integrals as suggested in Ref.³³⁾

On the other hand, the systematic FRR expansion of the nucleon mass is:

$$M_N = a_0^A + a_2^A m_\pi^2 + a_4^A m_\pi^4 + a_6^A m_\pi^6 + \sigma_{NN}^\pi(m_\pi, \Lambda) + \sigma_{N\Delta}^\pi(m_\pi, \Lambda) + \sigma_{\text{tad}}^\pi(m_\pi, \Lambda), \quad (2.9)$$

where the dependence on the *shape* of the regulator is implicit. The dependence on the value of Λ and the choice of regulator is eliminated, to the order of the series expansion, by fitting the coefficients, a_n^A , to lattice QCD data. The clear indication of success in eliminating model dependence and hence having found a suitable regularisation method, is that the higher order coefficients (a_i^A , $i \geq 4$) should be small and that the renormalised coefficients, c_i , and the result of the extrapolation should be insensitive to the choice of ultraviolet regulator. The forms of the $NN\pi$ and $N\Delta\pi$ contributions were given earlier, while the tadpole term has the form:

$$\sigma_{\text{tad}}^\pi = -\frac{3}{16\pi^2 f_\pi^2} c_2 m_\pi^2 \left\{ \int_0^\infty dk \left(\frac{2k^2 u^2(k)}{\sqrt{k^2 + m_\pi^2}} \right) - t_0 \right\}, \quad (2.10)$$

where in Eq. (2.10) t_0 , defined such that the term in braces vanishes at $m_\pi = 0$, is a local counter term introduced to ensure a linear relation for the renormalisation of c_2 .

The result of the fit to the latest two-flavor lattice QCD data for the mass of the nucleon is shown in Fig. 4, with the corresponding parameters given in Table I. It is remarkable that all four curves based on FRR are indistinguishable on this plot. Furthermore, we see from Table I that the coefficient of m_π^4 in all of those cases is quite small – an order of magnitude smaller than the dimensionally regularised forms. Similarly, the FRR coefficients of m_π^6 are again much smaller than their DR counterparts. This indicates that the residual series, involving a_i , is converging when the chiral loops are evaluated with a FRR.

Regulator	a_0	a_2	a_4	a_6	Λ	χ^2/dof
Dim. Reg.	0.827	3.58	3.63	-0.711	-	0.43
Dim. Reg. (BP)	0.792	4.15	8.92	0.384	-	0.41
Sharp Cutoff	1.06	1.47	-0.554	0.116	0.4	0.40
Monopole	1.74	1.64	-0.485	0.085	0.5	0.40
Dipole	1.30	1.54	-0.492	0.089	0.8	0.40
Gaussian	1.17	1.48	-0.504	0.095	0.6	0.40

Table I. Bare, unrenormalised, parameters extracted from the fits to lattice data displayed in Fig. 4 – from Ref.¹⁸⁾ All quantities are in units of appropriate powers of GeV and $\mu = 1$ GeV in Eq. (2.8).

The corresponding, physically meaningful, renormalized coefficients are shown in Table II, in comparison with the corresponding DR coefficients found using Eq. (2.8). Details of this renormalisation procedure are given in Ref.³²⁾ The degree of consis-

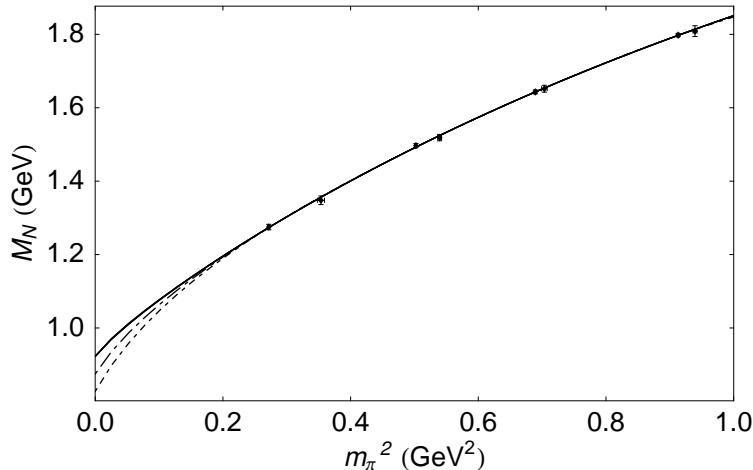


Fig. 4. Fits to lattice data for various ultra-violet regulators including the tadpole term – from Ref.¹⁸⁾ The sharp cut-off, monopole, dipole and Gaussian cases are depicted by solid lines, **indistinguishable** on this plot. The dimensional regularised forms are illustrated by the dash-dot curves, with the correct branch point corresponding to the higher curve. Lattice data is from Ref.²⁶⁾

Regulator	c_0	c_2	c_4
Dim. Reg.	0.827(120)	3.58(50)	3.6(15)
Dim. Reg. (BP)	0.875(120)	3.14(50)	7.2(15)
Sharp cutoff	0.923(130)	2.61(66)	15.3(16)
Monopole	0.923(130)	2.45(67)	20.5(30)
Dipole	0.922(130)	2.49(67)	18.9(29)
Gaussian	0.923(130)	2.48(67)	18.3(29)

Table II. Renormalised expansion coefficients in the chiral limit obtained from various regulator fits to lattice data – from Ref.¹⁸⁾ (All quantities are in units of appropriate powers of GeV.) Errors are statistical in origin arising from lattice data. Deviations in the central values indicate systematic errors associated with the chiral extrapolation.

tency between the best-fit values found using all choices of FRR is remarkably good. On the other hand, DR significantly underestimates c_4 . We can understand the problem very simply; it is not possible to accurately reproduce the necessary $1/m_\pi^2$ behaviour of the chiral loops (for $m_\pi > \Lambda$) with a 3rd order polynomial in m_π^2 .

It is clear that the use of an EFT with a FRR enables one to make an accurate extrapolation of the nucleon mass as a function of the quark mass. Indeed, all of the FRR used yield physical nucleon masses that lie within a range of 1%. It is especially interesting to observe the very small difference between the physical nucleon masses obtained with each FRR when we go from LNA to NLNA – i.e., when the effect of the Δ is included. (The change is typically a few MeV for a FRR but more than 100 MeV for DR.) Once again the convergence properties of the FRR expansion are remarkable.

Regulator	LNA	NLNA	
	m_N	m_N	σ_N
Dim. Reg.	0.784	0.884 ± 0.103	50.3 ± 10.0
Dim. Reg. (BP)	0.784	0.923 ± 0.103	42.7 ± 10.0
Sharp cutoff	0.968	0.961 ± 0.116	34.0 ± 13.0
Monopole	0.964	0.960 ± 0.116	33.0 ± 13.0
Dipole	0.963	0.959 ± 0.116	33.3 ± 13.0
Gaussian	0.966	0.960 ± 0.116	33.2 ± 13.0

Table III. The nucleon mass, m_N (GeV), and the sigma commutator, σ_N (MeV), extrapolated to the physical pion mass obtained in a NLNA (fourth order) chiral expansion – from Ref.¹⁸⁾ Convergence of the expansion is indicated by the nucleon mass obtained in an analysis where we retain only the LNA (third order) behaviour.

§3. Variation of M_N Under a Chiral Invariant Scalar Field

In order to avoid large violations of chiral symmetry, it is most natural to suppose that in models such as QMC we are in a representation where $\bar{\psi}_N \psi_N$ is chiral invariant. For example, if one views the scalar, intermediate range NN interaction as the result of two pion exchange this is exactly what one would find. Within such a framework the mass of the pion is protected by chiral symmetry,³⁵⁾ even in medium, and one expects only very small deviations of the in-medium pion mass from its free value - at least for densities typical of normal nuclei. This theoretical expectation is certainly supported by recent pionic atom data.³⁴⁾

In order to draw conclusions about the scalar polarizability of the nucleon the issue to be addressed is then simply: how does the mass of the nucleon change when the quark mass varies, $m_q \rightarrow m_q^* \equiv m_q - g_\sigma^q \sigma$, with the pion mass kept fixed? The extensive studies of the nucleon mass in lattice QCD and especially the success in relating full and quenched lattice QCD simulations,³⁶⁾ give us confidence that we understand the pion loop contributions. In particular, it was found in Ref.³⁶⁾ that the coefficients a_i were the same, within fitting errors, in full and quenched QCD when we used a dipole regulator with mass 0.8 GeV – in the case of both the N and the Δ . We note that the separation of the pion loop contributions is model dependent, unlike the extraction of the renormalized coefficients, c_i , where we were careful to establish the model independence at the 1% level. However, the possibility of establishing a connection between QCD and fundamental properties of nuclear systems, such as saturation, is so important that it seems worthwhile to tolerate a degree of model dependence at this stage.

The free nucleon mass expansion in free space:

$$M_N = a_0 + a_2 m_\pi^2 + a_4 m_\pi^4 + \text{self-energy}(m_\pi, \Lambda) \quad (3-1)$$

then becomes

$$M_N^* = a_0 + a_2 m_\pi^{*2} + a_4 m_\pi^{*4} + \text{self-energy}(m_\pi, \Lambda) \quad (3-2)$$

in-medium. As noted above, we use a dipole regulator of mass 0.8 GeV for the pion loops, which do not change in-medium because the pion mass is protected by chiral

symmetry. To lowest order the GMOR relation gives $m_\pi^{*2} \propto m_q^*$. However, since the scalar potential is not necessarily small, we need to keep the next order term in order to extract the dependence of the nucleon mass in-medium on the effective quark mass.

In χ Pt the next term is non-analytic in m_q .³⁷⁾ However, over the relevant mass range, fits to lattice data, as well as fits to Schwinger-Dyson phenomenology^{38),39)} and a best fit to the χ Pt expansion, all suggest that

$$m_\pi^2 \approx 4m_q + 20m_q^2, \quad (3.3)$$

with all masses in GeV.

If we now replace the quark mass, m_q , by $m_q^* \equiv m_q - g_\sigma^q \sigma$, to second order in σ one finds $M_N^* = M_N - (4a_2 g_\sigma^q) \sigma + (20a_2 + 16a_4)(g_\sigma^q)^2 \sigma^2$, which can be written as $M_N^* - M_N \approx g_\sigma(1 - g_\sigma \sigma) \sigma$, if we use the numerical values of $a_{2,4}$ from the analysis reported in Sec. 2.2 (without the tadpole). That is, $g_\sigma \sigma \approx -g_\sigma^2$ and the reduction of the effective σ -nucleon coupling at nuclear matter density, where $g_\sigma \sigma \in (150, 200)$ MeV is around 15-20 %. This is in remarkable agreement with the upper end of the values found phenomenologically in the QMC model.

If instead of the values found in Sec. 2.2 one used the more recent fit of Table I (including the tadpole term), the coefficient of g_σ^2 in the expression for $g_\sigma \sigma$ would be -0.6 instead of -1. This is in remarkable agreement with the value given by the bag model ($g_\sigma \sigma = -0.11 R g_\sigma^2$, with $R = 1\text{fm} = 5\text{GeV}^{-1}$). In terms of the phenomenological role of $g_\sigma \sigma$ in nuclear saturation, the difference between these two estimates is unimportant.

To summarize, the FRR expansion of the nucleon mass in terms of quark mass, with parameters determined by fits to the best two-flavor, lattice QCD simulations, leads to a scalar polarizability of the sign and magnitude found in the QMC model. Amongst the natural consequences of this result, as we explained in the Introduction, is that nuclear matter will naturally saturate as the density increases. Thus in a very meaningful sense the present result connects the saturation of nuclear matter to the structure of the nucleon itself within QCD.

§4. Conclusion

The remarkable progress in resolving the problem of chiral extrapolation of lattice QCD data, in the case (such as the nucleon mass) where the chiral coefficients are known accurately, gives one confidence that the pion loop contributions are under control. In the case of the nucleon one can use this control to estimate the effect of applying a chiral invariant scalar field to the nucleon – i.e. to estimate the so-called “scalar polarizability” of the nucleon. We stress that, unlike the determination of low energy coefficients, which is demonstrably model independent, for the present the determination of the scalar polarizability requires a choice of regulator. We chose a dipole of mass 0.8 GeV because of the connection between full and quenched QCD that has been established in this case. The resulting value is in excellent agreement with the range found in the quark-meson coupling model (QMC), which has provided an impressive description of many phenomena in nuclear physics. Of most im-

diate significance is the fact that such a scalar polarizability very naturally yields nuclear saturation within a relativistic mean field treatment of nuclear matter. Thus in a very real sense the results presented here provide a direct connection between our growing power to compute hadron properties from QCD itself and fundamental properties of atomic nuclei. This is especially interesting in the light of recent experimental evidence^{43)–45)} that the structure of a bound “nucleon” differs from that observed when it is free.^{40)–42)} These are important problems that will be more and more a focus for our field in the coming years.

Acknowledgements

This work is supported by the Australian Research Council and by DOE contract DE-AC05-84ER40150, under which SURA operates Jefferson Laboratory.

References

- 1) C. J. Benesh, T. Goldman and G. J. . Stephenson, Phys. Rev. C **68**, 045208 (2003) [arXiv:nucl-th/0307038].
- 2) J. R. Smith and G. A. Miller, Phys. Rev. Lett. **91**, 212301 (2003).
- 3) P. A. M. Guichon, Phys. Lett. B **200**, 235 (1988).
- 4) K. Saito and A. W. Thomas, Phys. Lett. B **327**, 9 (1994) [arXiv:nucl-th/9403015].
- 5) K. Saito and A. W. Thomas, Phys. Rev. C **51**, 2757 (1995) [arXiv:nucl-th/9410031].
- 6) P. A. M. Guichon, K. Saito, E. N. Rodionov and A. W. Thomas, Nucl. Phys. A **601**, 349 (1996) [arXiv:nucl-th/9509034].
- 7) W. Bentz and A. W. Thomas, Nucl. Phys. A **696**, 138 (2001) [arXiv:nucl-th/0105022].
- 8) G. Chanfray, M. Ericson and P. A. M. Guichon, Phys. Rev. C **68**, 035209 (2003) [arXiv:nucl-th/0305058].
- 9) G. Hellstern, R. Alkofer and H. Reinhardt, Nucl. Phys. A **625**, 697 (1997) [arXiv:hep-ph/9706551].
- 10) B. D. Serot and J. D. Walecka, Int. J. Mod. Phys. E **6**, 515 (1997) [arXiv:nucl-th/9701058].
- 11) P. A. M. Guichon and A. W. Thomas, arXiv:nucl-th/0402064.
- 12) T. Lippert, S. Gusken and K. Schilling, Nucl. Phys. Proc. Suppl. **83** (2000) 182.
- 13) C. W. Bernard *et al.*, Phys. Rev. D **64** (2001) 054506 [arXiv:hep-lat/0104002].
- 14) L. F. Li and H. Pagels, Phys. Rev. Lett. **26**, 1204 (1971).
- 15) T. Hatsuda, Phys. Rev. Lett. **65**, 543 (1990).
- 16) S. Durr, arXiv:hep-lat/0208051.
- 17) R. E. Stuckey and M. C. Birse, J. Phys. G **23**, 29 (1997) [arXiv:hep-ph/9602312].
- 18) D. B. Leinweber, A. W. Thomas and R. D. Young, to appear in Phys. Rev. Lett. , arXiv:hep-lat/0302020.
- 19) H. Pagels, Phys. Rept. **16**, 219 (1975).
- 20) J. Gasser, M. E. Sainio and A. Svarc, Nucl. Phys. B **307**, 779 (1988).
- 21) R. F. Lebed, Nucl. Phys. B **430**, 295 (1994) [arXiv:hep-ph/9311234].
- 22) M. K. Banerjee and J. Milana, Phys. Rev. D **54**, 5804 (1996) [arXiv:hep-ph/9508340].
- 23) S. V. Wright, PhD thesis, University of Adelaide, 2002.
- 24) A. W. Thomas, Adv. Nucl. Phys. **13**, 1 (1984).
- 25) G. P. Lepage, arXiv:nucl-th/9706029.
- 26) A. Ali Khan *et al.* [CP-PACS Collaboration], Phys. Rev. D **65**, 054505 (2002) [Erratum-ibid. D **67**, 059901 (2003)] [arXiv:hep-lat/0105015].
- 27) S. Aoki *et al.* [JLQCD Collaboration], Phys. Rev. D **68**, 054502 (2003) [arXiv:hep-lat/0212039].
- 28) Y. Iwasaki, Nucl. Phys. B258 (1985) 141.
- 29) UKQCD, C.R. Allton *et al.*, Phys. Rev. D60 (1999) 034507, hep-lat/9808016.
- 30) R. Sommer, Nucl. Phys. B411 (1994) 839, hep-lat/9310022.
- 31) R.G. Edwards, U.M. Heller and T.R. Klassen, Nucl. Phys. B517 (1998) 377, hep-lat/9711003.

- 32) R. D. Young, D. B. Leinweber and A. W. Thomas, *Prog. Part. Nucl. Phys.* **50**, 399 (2003) [arXiv:hep-lat/0212031].
- 33) J. F. Donoghue, B. R. Holstein and B. Borasoy, *Phys. Rev. D* **59**, 036002 (1999) [arXiv:hep-ph/9804281].
- 34) P. Kienle and T. Yamazaki, *Prog. Part. Nucl. Phys.* **52** (2004) 85.
- 35) W. Bentz, A. Arima and H. Baier, *Annals Phys.* **200**, 127 (1990).
- 36) R. D. Young, D. B. Leinweber, A. W. Thomas and S. V. Wright, *Phys. Rev. D* **66**, 094507 (2002) [arXiv:hep-lat/0205017].
- 37) J. Gasser and H. Leutwyler, *Nucl. Phys. B* **250**, 465 (1985).
- 38) P. Maris and P. C. Tandy, *Phys. Rev. C* **60**, 055214 (1999) [arXiv:nucl-th/9905056].
- 39) P. Maris and C. D. Roberts, *Phys. Rev. C* **56**, 3369 (1997) [arXiv:nucl-th/9708029].
- 40) D. H. Lu, K. Tsushima, A. W. Thomas, A. G. Williams and K. Saito, *Phys. Rev. C* **60** (1999) 068201 [arXiv:nucl-th/9807074].
- 41) D. H. Lu, A. W. Thomas and A. G. Williams, *Phys. Rev. C* **57**, 2628 (1998) [arXiv:nucl-th/9706019].
- 42) A. W. Thomas, D. H. Lu, K. Tsushima, A. G. Williams and K. Saito, arXiv:nucl-th/9807027.
- 43) S. Strauch *et al.* [Jefferson Lab E93-049 Collaboration], *Phys. Rev. Lett.* **91** (2003) 052301 [arXiv:nucl-ex/0211022].
- 44) S. Dieterich *et al.*, *Phys. Lett. B* **500**, 47 (2001) [arXiv:nucl-ex/0011008].
- 45) K. G. Fissum *et al.* [Jefferson Lab Hall A Collaboration], arXiv:nucl-ex/0401021.